

PAPER • OPEN ACCESS

3D stability analyses of Skjeggestad landslide

To cite this article: H P Jostad *et al* 2021 *IOP Conf. Ser.: Earth Environ. Sci.* **710** 012005

View the [article online](#) for updates and enhancements.

You may also like

- [Comparative Study on Calculation Methods for Stability Evaluation Based on BIM Models of Soil Landslides](#)
Cheng Wei, Jinbao Wang and Feng Cheng
- [A Study of the Relationship between Fractal Dimension of Boundary Trace and Stability of the Loess-bedrock Landslide](#)
Bo Wu, Fa Suo Zhao, Shao Yan Wu et al.
- [Structuring the Environment of Landslide-Prone Disaster and Its Mitigation in The District of Banyumanik](#)
H Tjahjono, S Suripin and K Kismartini



The Electrochemical Society
Advancing solid state & electrochemical science & technology

242nd ECS Meeting

Oct 9 – 13, 2022 • Atlanta, GA, US

Abstract submission deadline: **April 8, 2022**

Connect. Engage. Champion. Empower. Accelerate.

MOVE SCIENCE FORWARD



Submit your abstract



3D stability analyses of Skjeggstad landslide

H P Jostad¹, N Sivasithamparam¹, S Lacasse¹, S A Degago⁵, T M H Le¹, S Giese²,
A Rosenquist af Åkershult³, T Johansen⁴ and R Aabøe⁵

¹ Norwegian Geotechnical Institute (NGI), Oslo, Norway

² Multiconsult AS, Oslo Norway

³ Trimble Solutions Gothenburg AB, Stockholm, Sweden

⁴ Geovita AS, Sandvika, Norway

⁵ Norwegian Public Roads Administration (NPRA), Oslo/Trondheim Norway

Corresponding author: suzanne.lacasse@ngi.no

Abstract. In 2015, a sudden landslide caused the failure of one of the pillars supporting the southern lanes of the Skjeggstad Bridge near Mofjellbekken on Expressway E18. The transportation corridor was closed to traffic for 17 months. To investigate the cause of the failure, an assessment of slope stability is necessary. Usually, limit equilibrium analysis of the middle two-dimensional (2D) cross-section is modelled. The Skjeggstad landslide geometry was not close to a 2D case, and three-dimensional (3D) modelling is more appropriate to analyse the slope. The paper calculates the stability of the slope that failed and compares the results of 3D finite element analyses with classical limit equilibrium and 2D finite element analyses. The analyses were run in the Novapoint GeoSuite Stability software. The soil parameters, including their statistical values, were obtained with the GeoSuite Soil Data Interpretation (SDI) module. A companion paper at this conference analyses the pillar neighbouring the landslide with the module GeoSuite Piles. The paper illustrates the importance of 3D effects in a stability analysis. The results of the analyses also illustrate the need to include appropriate consideration of any strain-softening and spatial variation of soil properties.

1. Introduction

In February 2015, an unexpected landslide occurred near Mofjellbekken, causing the failure of a large bridge pillar along the main transportation corridor between Oslo and southern Norway. Traffic chaos ensued for a period of 17 months. This paper focuses on three-dimensional (3D) analysis of the landslide that caused the failure of one of the bridge pillars. A companion paper [1] studies the capacity of the adjacent pillar foundation.

Engineering design on soft Norwegian clay always represents a challenge. The design software Novapoint GeoSuite (www.geosuite.se), designed for practice, was used to provide visualisation, soil data interpretation and geotechnical calculation platform to establish a common ground for the analyses if both stability and pile group design. The aim of the present paper is to demonstrate the importance of accounting for 3D effects for the evaluation of slope stability in general, and for the Skjeggstad landslide in particular. In addition, the effect of strain softening of the quick clay is discussed.

The paper describes briefly the failure that occurred, discusses the interpretation of the undrained shear strength in GeoSuite and compares and discusses the results of the 2D and 3D stability analyses.



2. The Skjeggstad Bridge landslide

The Skjeggstad Bridge (also called Mofjellbekken) was built between 1998 and 2001. A fill (called "old fill") was placed in the area before 2006 and covered the slope under study. In 2015, a "new" fill was placed on the crest of the slope that failed. The landslide occurred on February 2, 2015 and damaged the southern lane of the bridge. Figure 1 shows the extent of the 10 000 m³ landslide [2]. Fortunately, the traffic (visible at the top of Fig. 1) was stopped immediately, and no lives were lost.



Figure 1. Photograph of the Skjeggstad Bridge landslide (view from the south) (Photo: Orbiton)

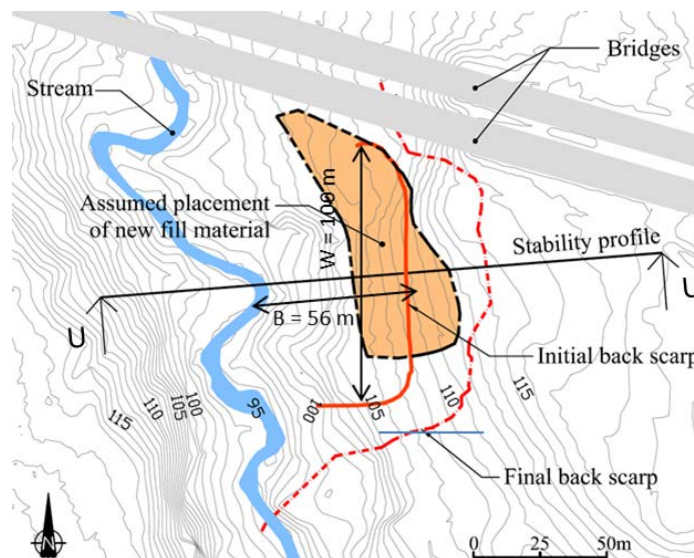


Figure 2. Topography before the landslide, new fill placed on top of slope (assumed location), assumed initial back-scarp and observed final back-scarp of landslide, location of the stream at bottom of the slope and cross-section U-U.

The Norwegian Water Resources and Energy Directorate (NVE) established an independent investigation commission to determine the cause of the landslide. Possible triggers investigated included: erosion from the stream, rainfall, traffic vibrations and the "new" fill material placed on the slope. The commission concluded that the new fill material placed on the slope crest immediately before the failure caused the landslide and failure of the bridge pillar [2] (Fig. 2). However, the shape and thickness of the new fill placed on top of the dry crust, are somewhat uncertain [3].

The topography in the area is complex. Figure 3 summarizes the zonation used in this study based on the piezocone tests run after the landslide. The soil layering consists of a dry crust of varying thickness underlain by a soft to medium soft silty sensitive clay. The clay is quick in some locations. Bedrock or stiff till underlies the clay. The depth to bedrock varies significantly. Figure 3 shows the extent of the landslide and the cross-sections U-U and Q-Q used for the early stability analyses ([2]; [3]).

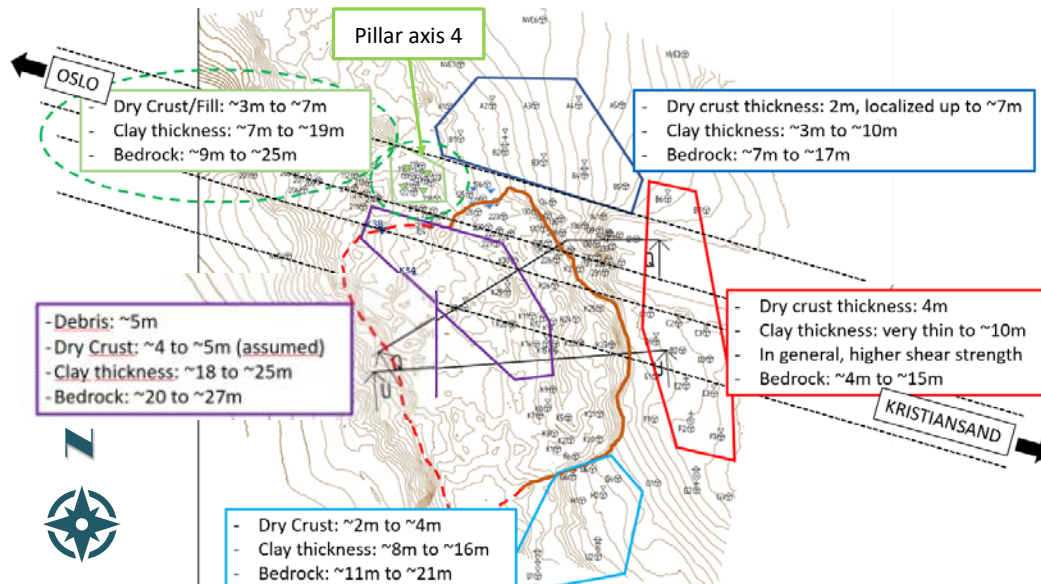


Figure 3. Overview of soil layering in different zones around the landslide

Figure 4 reproduces the profile and critical failure surfaces from early stability analyses of cross-section U-U [2];[3]. A factor of safety (F) of 1.17 was obtained before the new fill was placed on the slope, using 2D limit equilibrium analysis. The safety factor reduced to 0.99 after the new fill was placed. Other stability analyses can be found in [4] and [5].

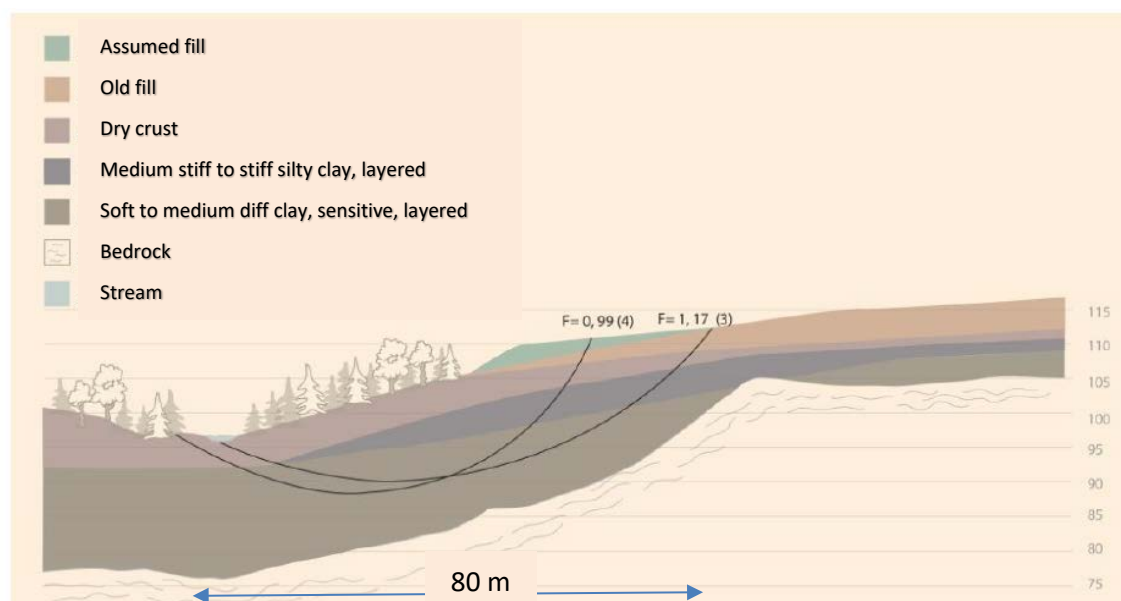


Figure 4. Critical failure surface in earlier 2D limit equilibrium analyses, cross-section U-U[2];[3]

Uncertainties in the analyses in Figure 4 include, in addition to the fill geometry, shear strength distribution, shape of failure surface, 3D effects, strain-softening and progressive failure mechanism.

Since this type of analysis is only an approximation for this complex case of stability, the fact that classical limit equilibrium or finite element 2D analyses give a safety factor close to 1 is only fortuitous.

3. 2D and 3D stability analyses

The stability of slopes is traditionally calculated using two-dimensional (2D) limit equilibrium methods (LEM) assuming a perfect plastic behaviour of the soil ([6]; [7]; [8]; [9]; [10]) The factor of safety (denoted FoS) is the maximum value by which the undrained shear strength can be divided before the driving forces from the weight of the soil mass and other external loads within the volume limited by a critical failure surface becomes larger than the stabilizing forces. In the last 20 years, the finite element method (FEM) has been increasingly used to model all types of geotechnical problems, including the stability of slopes. Comparisons of LEM and FEM analyses for slopes were presented in [11].

Compared to classical LEM, the benefits of using FEM for the analysis of slopes include: (1) FEM finds the most critical failure mechanism without prior assumptions of the shape and location of the slip surface, kinematics, internal stresses or mobilization, moment equilibrium etc; (2) FEM can account for aspects of soil behaviour such as dilatancy, strain-softening, load history effects, stress path dependency, strain rate effects, anisotropy etc; and (3) FEM can easily be extended to account for complex 3-dimensional (3D) effects. On the other hand, there are also challenges; (1) FEM calculations require significantly longer time; (2) FEM analyses need input on the soil stress-strain properties such as moduli, dilatancy, softening parameters, etc; (3) FEM results can be mesh-dependent, i.e. overshoot due to discretisation limitations and non-uniqueness due to strain-softening; (4) FEM may terminate due to numerical difficulties to achieve equilibrium; and (5) with FEM, it can prove difficult to calculate the factor of safety along predefined slip surfaces that are different from the most critical surface.

The main objective of the paper is to demonstrate the effect of 3D modelling on the FoS obtained with a 2D model. It is important to realise that a back-calculation of a failure with 2D LEM or FEM should not give an FoS of 1 because such analysis does not account for 3D effects nor behavioural aspects such as strain-softening. Obtaining an FoS of 1 at failure with 2D analyses is therefore not an indication that the method of calculation is reliable or representative.

4. Soil parameters for stability analysis

The key input data to the stability analyses include topography, soil layering, shear strength and unit weights of soil and fill material. The interpretation of the parameters was done in the GeoSuite Soil Data Interpretation (SDI) module. The information from the earlier site investigations during the construction of the bridge [12] and those carried out after the landslide were used. Where possible, a statistical analysis of the soil parameters was done (mainly for cone resistance data from piezocone tests (CPTU) after the landslide). When data were not available, the parameters were deduced from correlations available in the SDI module. Table 1 presents the parameters established for the stability analyses.

4.1 Index properties

All the index properties were obtained from the site investigation (both *in situ* and laboratory tests) prior to the construction of the bridge [12]. Except for the sensitivity, the measured index properties were essentially constant with depth. The plasticity index of 5 to 8% in the quick clay is extremely low, suggesting very high stress-induced anisotropy.

4.2 Undrained shear strength

Figure 5 presents the results of the undrained shear strength interpreted from the piezocone tests (CPTU) in each of the five zones in Figure 3. The CPTU undrained shear strength corresponds to the triaxial compression strength (s_{uTC}) in the laboratory. Figure 6 gives the mean \pm one standard deviation in each of the five zones. The coefficient of variation (COV = ratio of one standard deviation to the mean) was about 15 to 20% below 7 m but could be as high as 30 % in the dry crust. Figure 7 compares the mean $s_{uTC(CPT)}$ in the five zones and Figure 8 shows the results of *in situ* vane shear (VS) tests run before the failure. The s_{uVS} is much lower than the $s_{uTC(CPT)}$: s_{uVS} is usually close to the average of TC and TE strengths and is thus expected to be lower than the $s_{uTC(CPT)}$. There is also a significant difference in the

shear strengths in the different locations, and the depth to bedrock/till. The same average shear strength was used in all analyses to ease a comparison of the geometrical effects in the 2D and 3D analyses.

Table 1. Summary of interpreted soil parameters for the stability analyses

Soil property	Crust (0-5 m)	Soft clay (2-19 m)	Source of data
Index properties			
Water content, w	25%	30%	Initial investigations, 3 boreholes
Plasticity index, I_p	10%	5-8%	Initial investigations, 3 boreholes
Sensitivity, S_t	4-10	75-150 (30 from 17m)	Initial site investigations, VS and fall cone
Clay content	--	30-35%	Initial investigations, 2 boreholes
Total unit weigh, γ_t	19.5 kN/m ³	19.5 kN/m ³	Initial investigations, 3 boreholes
Undrained shear strength, s_u			
TC (from CPTU), $s_{uTC(CPTU)}$	--	Figure 5	CPTU tests ($N_{kt} = 10-14$)
Average (from VS), s_{uVS}	30-60 kPa	Figure 5	Only a few VS tests
Anisotropy ratio s_{uTC}/s_{uDSS}	1.6	1.7	
Anisotropy ratio s_{uTE}/s_{uDSS}	0.5	0.45	Used correlations in SDI [13]; [14]
Notation TC = Triaxial compression	TE = Triaxial extension	DSS = Simple shear	
CPTU= test	VS = Vane shear	p'_o = In situ effective overburden stress	

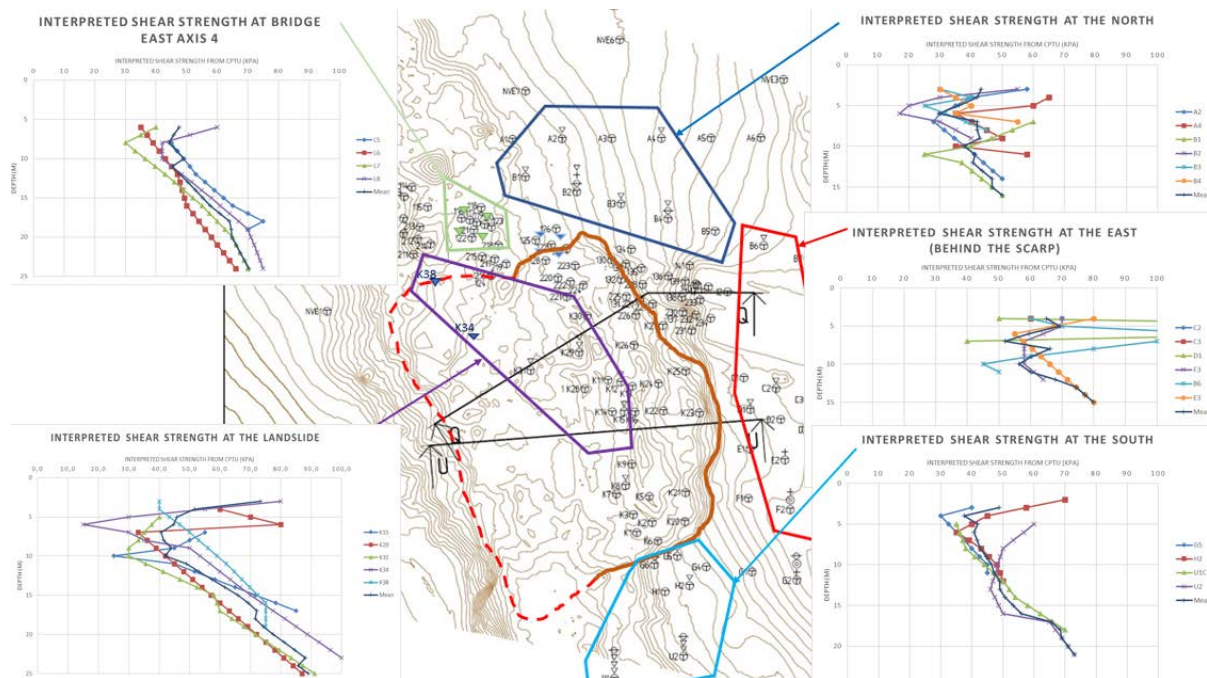


Figure 5. Undrained triaxial compression shear strength profiles interpreted from CPTU in five zones

4.3 Stress history

There were very few oedometer tests to estimate the pre-consolidation stress and overconsolidation ratio (OCR). The OCR was obtained from the undrained shear strength ratio in triaxial compression normalized with the effective overburden stress and comparing it with values for Norwegian clays and other soft clays in the literature ([13]; [14]). The inferred OCR is therefore only approximate. Nonetheless, it was possible to obtain a reasonably realistic approximate OCR profile with depth [1]. The OCR in the crust is greater than 3, and decreases from 3 to unity between depths of 5 to 19m.

5. 2D LEM and FEM analyses of stability

The Trimble Novapoint GeoSuite Toolbox (www.geosuite.se) [15] was used. The design software has a series of geotechnical calculation programs, including Stability, Settlement, Bearing Capacity, Piles and Excavation modules. For the 2D analyses, six 2D cross-sections were analysed (Fig. 9).

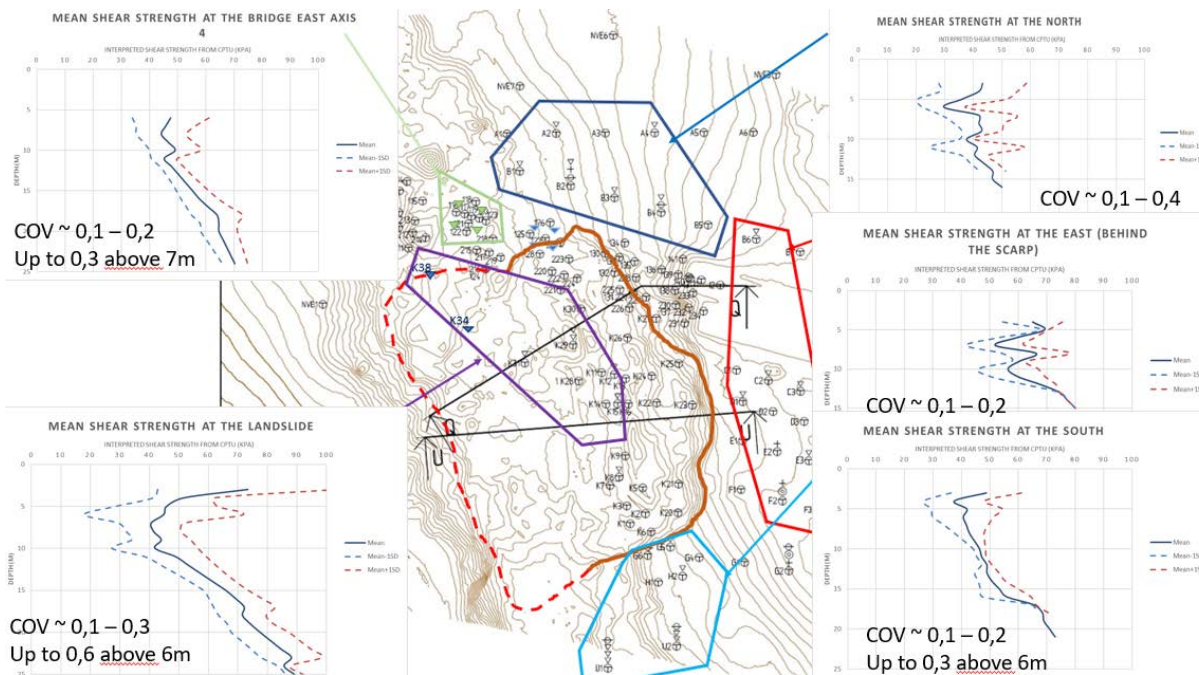


Figure 6. Mean ± one standard deviation of CPTU shear strength profiles in the five zones

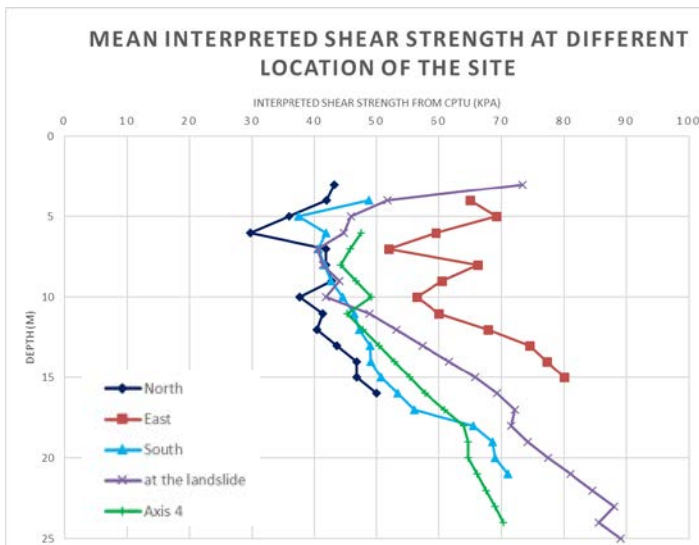


Figure 7. Comparison of mean $s_{u\ CPTU}$ at Skjeggestad site

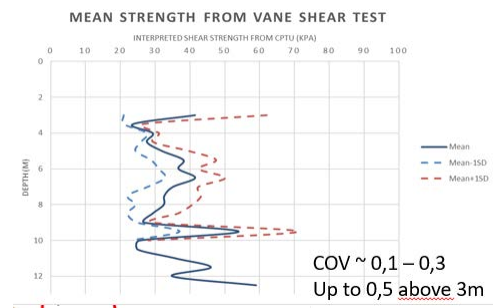


Figure 8. In situ VS strength

Figure 10 illustrates the slightly idealized geometry of the topography, soil layering and bedrock in cross-section U-U. This cross-section is located where the slope was steepest. The geometry of the new fill is approximate due to the uncertainties mentioned earlier. The calculated FoS was 0.85 assuming a circular slip surface limited by the bedrock. The slip surface starts at the back of the fill and ends up slightly at the outskirts of the toe of the slope.

The calculated critical slip surface follows the bedrock in several of the cross-sections, suggesting that assuming a circular slip surface will overestimate the FoS. The 2D LEM analyses showed that the FoS varied significantly from cross-section to cross-section. The highest FoS=1.38 was for cross-section 1-1 1 which is just outside of the failure footprint (Fig. 2). Cross-section Un-Un through the north side of the fill had an FoS of 1.07. It is not adequate to assume that the calculated FoS in section U-U is

representative for the landslide (see initial and final back-scarps in Fig. 2). One alternative, when doing 2D analyses of a 3D landslide geometry is to use a 'weighted average' FoS of several cross-sections within the failure volume. For the 4 sections crossing the landslide (Fig. 2), the average FoS was $(1.07 \times 0.25 + 0.86 \times 0.25 + 0.85 \times 0.25 + 0.95 \times 0.25) = 0.93$. In these LEM analysis, the effect of shear on the two out-of-plane sides of the slide is neglected. Since the critical slip surface varies from one cross-section to another, the displacement field would need to be continuous between each cross-section. The calculated FoS is thus expected to be significantly larger than the FoS=0.93 calculated above.

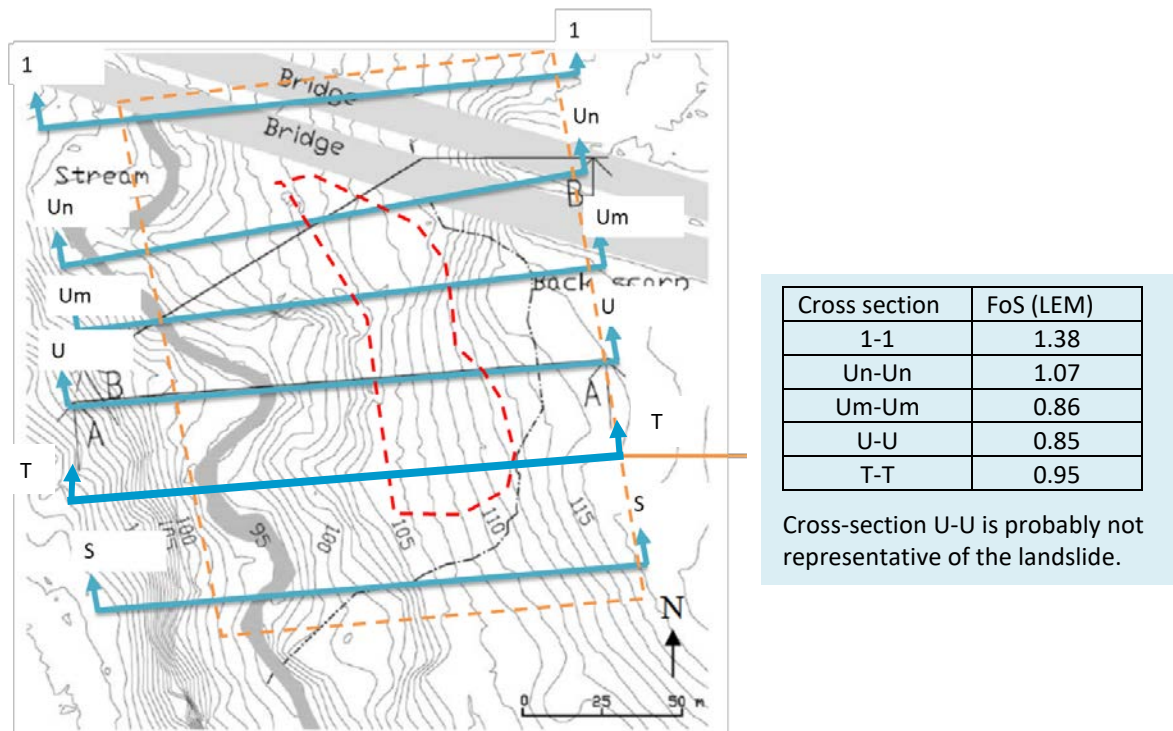


Figure 9. Cross-sections selected for 2D slope stability analyses

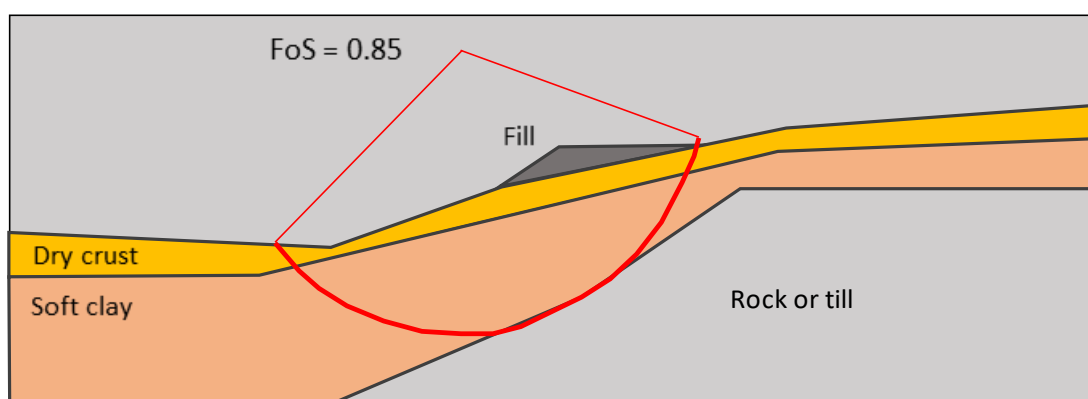


Figure 10. Critical slip surface with FoS=0.85 in GeoSuite Stability LEM analysis (cross-section U-U)

The 2D cross-sections analysed by LEM (Fig. 9) were also used for the FEM. In the GeoFuture research project (www.geofuture.no; [16]), the NGI FE program Bifurc was implemented in GeoSuite Stability. The same geometries and shear strength distributions were then used in both LEM and FEM analysis [17]. In the FEM analysis, the cross-sections were discretized by triangular 6-noded elements. Figure 11 gives an example of a discretized cross-section (element mesh) for section U-U. The mesh consisted of 464 elements and 1009 nodes. The vertical- and horizontal displacement at the nodes along

the bottom boundary were fixed while the nodes along the two vertical boundaries were fixed in the horizontal direction and free in the vertical direction. In the 2D FEM analyses, the nodal forces due to the weight of the soil and fill were first applied to the model. The calculated maximum nodal displacement in the mesh versus the scaling factor of the weight is shown in Figure 12 (left). Since the scaling factor is less than 1.0, the slope failed during application of the weight. The FoS is equal to the maximum load scaling factor of 0.87 which is slightly larger than the FoS=0.85 obtained by LEM. The effect of mesh discretization was further checked. A mesh with 1317 elements gave a FoS of 0.83, and a mesh of 2637 elements gave a FoS of 0.82, which is slightly lower than obtained by LEM. The discretization error using 464 elements is therefore estimated to be about 7%.

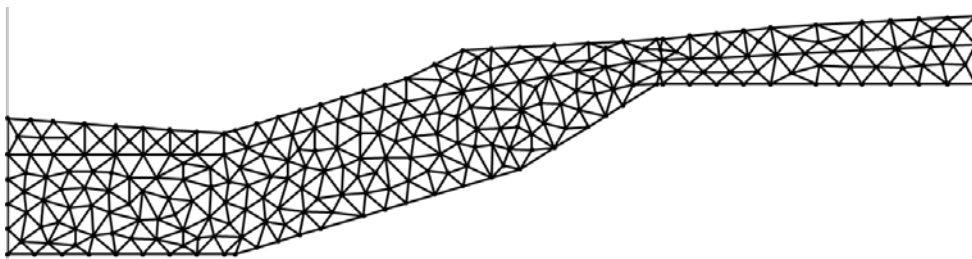


Figure 11. Example of 2D finite element mesh used for cross-section U-U

In cases where the FoS > 1.0, the undrained shear strengths are gradually reduced by dividing them by an increasing factor (FoS). This is done in increments with an equilibrium iteration for each increment (Fig. 12 (left)) for cross-section U-U). The scaling factor is automatically adjusted so the sum of all displacement increments in the mesh is kept constant during the iteration scheme. This solution procedure is generally called arch-length method. Figure 12 (right) shows the calculated maximum displacement in the mesh versus the reduction factor (FoS) during this calculation phase for cross-section 1-1. In total, 84 increments were required to find the FoS that corresponded to failure of the slope. The number of degrees of freedom (node displacements), increments and iterations and the calculation speed of the computer govern the calculation time. The calculation time was 10 minutes on a conventional PC using one CPU. Figure 13 illustrates the calculated failure mode for cross-section U-U with displacement vectors at failure. This failure mode agrees very well with the calculated LEM slip surface in Figure 10.

6. 3D FEM analyses of stability

6.1 3D effects using earlier calculated charts

Jostad and Lacasse [17] developed charts to estimate the increase in the FoS in a 3D analysis compared to a 2D plane-strain analysis ($F3D$). This chart, given in Figure 14, indicates that $F3D$ is a function of the height to width ratio (H/W) of the slope, the inclination of the critical part of the slope b and the normalized depth to a strong layer $d = D/H$ that limit the depth of the slip surface. For the Skjeggestad landslide, H was taken as 16 m, the bottom of the slip surface D as 10 m and the width of the initial slide W was estimated as 100 m. Thus, for H/W of 16/100, $b = 3$ and $d = 0.6$, through interpolation in Figure 14, an approximate 3D effect, $F3D$ of 1.12 was obtained. The $F3D$ of 1.12 means a 12% increase in 3D compared to 2D conditions. By multiplying this factor with the average 2D FoS from the four cross-sections, the FoS of the initial slide accounting for 3D effects becomes, FoS=0.93 x 1.12=1.04. This safety factor is only slightly larger than the factor of unity corresponding to failure. Azzouz and Baligh [18] also prepared charts comparing slopes under infinite strip and square loadings and concluded that the 3D effects were important.

6.2 New 3D FEM analyses

For the 3D analyses, the GeoSuite Toolbox was again used. The slope was first modelled using an idealized 3D model. With this idealisation, the most critical cross-section (U-U) was extruded in the y-direction to a width that correspond to the width of the initial slide. This width was estimated as 100 m (Fig. 2). Due to symmetry, only half of the total width was modelled. This volume was then

discretized with 2454 12-noded tetrahedral elements. The size of the tetrahedral elements corresponded to the elements in the 2D analysis using 464 6-noded triangular elements. The same overshoot (i.e. 7%) is expected in the 3D analysis. The FoS results given in this section do not account for this overshoot.

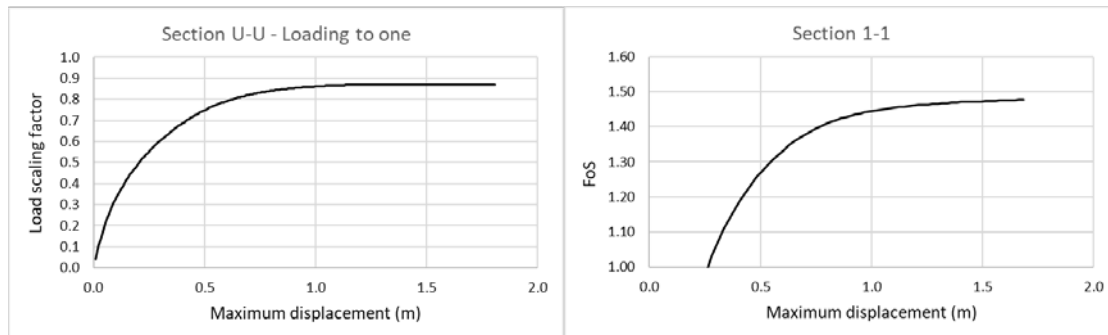


Figure 12. Calculated load scaling factor for section U-U (left) and (FoS) for section 1-1 (right)

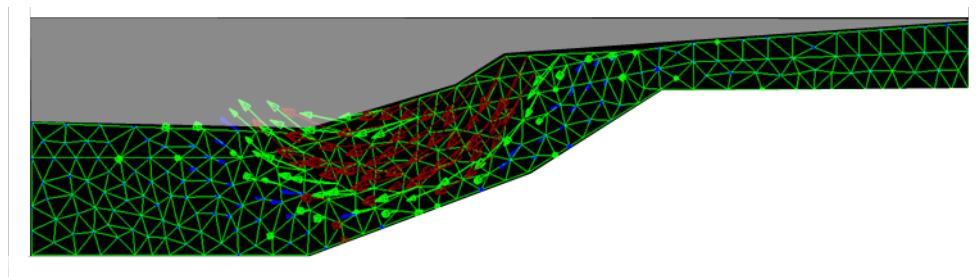


Figure 13. Calculated failure mode by 2D FEM for cross-section U-U (FoS=0.87)

The nodes at the external side boundary were fixed in the two horizontal directions and free in the vertical direction, while the nodes along the symmetry plane were fixed normal to the plane only. This prevents the failure mode to develop at the side of the model and the width of the calculated failure mode will be within the model and automatically include a realistic side shear at this boundary. The calculated FoS for the idealized 3D model was 0.97, an increase by 11% compared to 0.87. This 11% represents the contribution from side shear, which agrees with the 12% obtained from Figure 14.

Second, a full 3D FEM analysis was carried out where the actual 3D geometries of the topography, soil layering, rock surface and fill were modelled. This analysis automatically accounts for the variations of FoS for the different 2D cross-sections and the 3D effects due to the requirements of continuity of the displacement field between the different cross-sections and side shear at the two ends of the most critical failure mechanism. Figure 15 presents the idealized topography of the full 3D model. The contour lines and colour represent the elevation, and $y = 0$ the location of cross-section U-U. The calculated FoS for the full 3D FEM analysis was 1.22, which is 40% larger than the safety factor for the 2D FEM most critical cross-section (0.87), and 25% larger than the safety factor from the idealized 3D model (0.97). This demonstrates that the 3D effect may be significant in slope stability analyses.

The plan view of the calculated 3D failure (Fig. 16) shows an area extending only slightly north of Section U-U and partly south of Section S-S. The results indicate that the calculated (3D) initial back-scarp is located somewhat south of the assumed location (Fig. 2). The failure goes down to the bedrock-/till layer, and agrees rather well with the 2D cross-sections, at least in locations U-U and S-S. However, the landslide on the south side extends further south than the observed final back-scarp (Fig. 2). This may be explained if the shear strength distribution is somewhat higher in the southern part than the average shear strength profile used in the 3D analysis. Unfortunately, no data are available in that southern area.

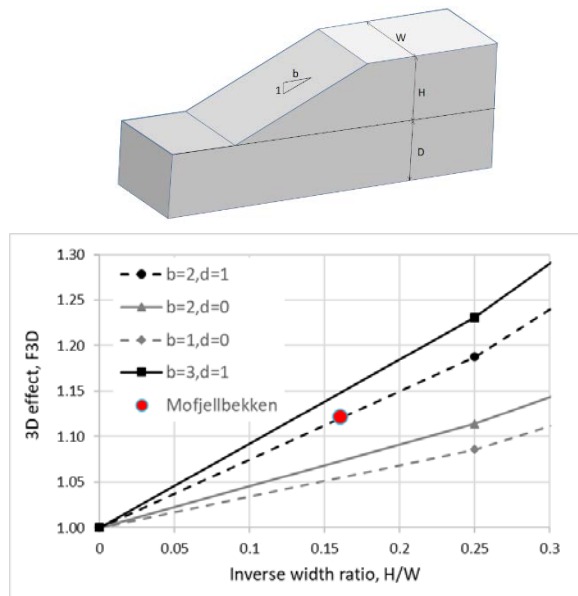


Figure 14. 3D effect on the 2D factor of safety as a function of width W , slope inclination b and normalized depth d [17]

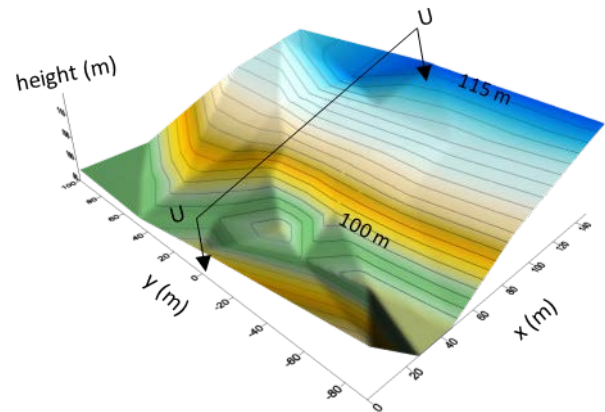


Figure 15. Idealized topography of 3D model without the new fill view3ed from the southwest, Section U-U is at $y=0$ (Fig. 2 shows and location of Section U-U)

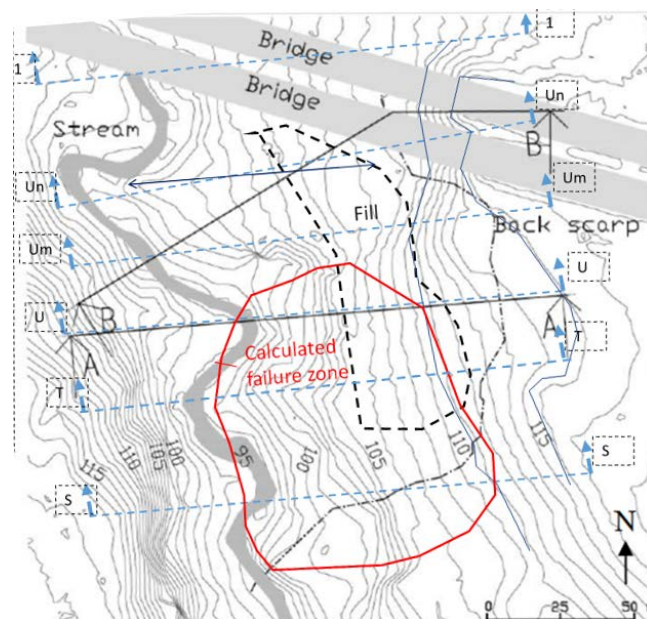


Figure 16. Extent of failure from full 3D analysis

6.3 Progressive failure due to strain softening

Based on the above calculations, the FoS of 1.22 is significantly higher than unity, which does not agree with the fact that a landslide did occur. There are uncertainties in the shear strength profiles, height and shape of the fill, but these are not large enough to explain the calculated discrepancy between the calculated FoS of 1.22 and the observed failure. However, the clay is sensitive which means that the strength will be reduced as shear strain increases after the shear stress has passed a peak value. By accounting for strain-softening in 2D FEM analysis, Rød vand et al. [5] suggested that the calculated FoS in cross-section U-U reduces due to strain-softening. In a sensitivity study of the effect of strain-

softening in design of fills in gently inclined areas with soft sensitive clays, Jostad et al. [19] found that the FoS can be reduced by more than 30% in a 2D cross-section of a slope. The effect of strain-softening is expected to be even larger for the 3D geometry considered. One therefore needs to account for the effect of progressive failure of strain-softening soils in stability analysis.

An increase in the safety factor to account for strain-softening is for example the adopted approach in Norway for designs related to road constructions ([20];[21]). The Norwegian Public Road Administration (NPRA) technical specification document N200 [21] requires an increase in the material factor to account for strain-softening.

6.4 Discussion

The 2D and 3D analyses herein illustrate that one can learn more from 3D slope stability analyses than from 2D analyses alone. It is beneficial to do the 3D analyses, but perhaps even more refinements are needed to enable a completely realistic safety factor in case of a failure (FoS = 1.0), such as the modelling of strain-softening, the spatial variability of the soil properties etc. Most importantly, the 3D analyses tell us that the earlier 2D classical limit equilibrium and FEM analyses giving a factor of safety close to 1 at failure, must owe this result to compensating errors with incomplete modelling of the complete problem at hand, including modelling of the characteristics of the landslide, the soil parameters and their spatial variability and the behaviour of the soil material(s) under increasing shear stress and shear strain.

When slopes fail, there is the need to understand the mechanisms and reasons for failure. This is done with back analyses, where a correct modelling of the problem is crucial to explain the observations. One therefore needs to take into account the 3D effect and strain softening behaviour to explain failures in slopes in sensitive clays. The 3D effect increases the safety factor while strain softening reduces it. This also implies that safety factors with analyses that do not include these two effects are probably fortuitous.

Key observations from this study of the Skjeggstad landslide include:

- For back-analysis, one needs to take into account, where relevant, 3D effects and strain-softening behaviour in order to explain observed displacements and collapse.
- In design, it is important to be cautious when examining calculated safety factors, understanding what has been modelled and the features of the actual behaviour that have not been included in the analyses, to ensure that one errs on the safe side when estimating factors of safety.
- Strain-softening played an important role in the onset and extent of the landslide because of the quick clay. Strain-softening can reduce the safety factor significantly [19].
- The authors believe that a full 3D analysis of the Skjeggstad landslide accounting for the strain-softening behaviour would give a FoS closer to unity.

7. Conclusions

The paper illustrated the benefit of accounting for 3D effects in slope stability analysis with the 2015 Skjeggstad Bridge landslide case study. The work demonstrates that for the Skjeggstad landslide, the 3D effects were significant (up to 40% increase on the factor of safety of the most critical 2D cross-section). One needs to take this into account to realistically explain the observed failure. However, for design in sensitive clays, one should be careful to fully utilize this 3D effect, because the calculated FoS can be reduced significantly due to strain-softening. The FEM (2D or 3D) is a very convenient tool that helps understand complex failure mechanisms of landslides including 3D geometrical effects, strain softening behaviour and progressive failure.

Slope stability analysis with a 3D FEM provides several benefits: 1) it finds a more accurate location of the slip surface (in 2D and LEM analyses, the location is decided "a priori"); 2) it accounts for the effects of 3D topography, soil layering and spatial distribution of the material properties; 3) it can use models that can include key soil characteristics such as stress dependency, load history, dilatancy and strain-softening; 4) it has been used for other geotechnical problems for more than 30 years; 5) the current user-interfaces make the approach easier to use than before; and 6) the computers have become significantly faster than earlier.

Acknowledgment

The work is part of the GeoFuture II project funded by The Research Council of Norway. The executing and sponsoring consortium includes NGI, GeoVita AS, Multiconsult AS, Norconsult AS, Rambøll AS, Cowi AS, SwecoAS, SINTEF Community, the Norwegian University of Science and Technology (NTNU), the Norwegian Public Roads Administration (NPRA), the Norwegian National Rail Administration, Trimble AS and AG Programutveckling Ekonomisk förening (AGEF). The authors thank NPRA for the permission to use this case study and for providing the soil parameter raw data. The authors also thank Mr C.H. Yan, Geotechnical Engineering Office (GEO), Civil Engineering and Development Department, Hong Kong, for his contributions to the study.

References

- [1] Bendovski R, Hetland R, Chen Y, Giese S, Rosenquist, AaÅ, Lacasse S, Johansen, T, Aasbøe, R and Degago, SA. (2021). Back-calculation of pillar foundation for Skjeggestad Bridge. NGM2021 (this conference).
- [2] NVE (Norwegian Water Resources and Energy Directorate) (2015). Skredet ved Mofjellbekken bruer (Skjeggestadskredet). Utredning av teknisk årsaks-sammenheng. Rapport 53/2015.
- [3] Haugen SB, Henderson LA and Amdal ÅMW (2016). Case-study of a quick clay landslide that caused the partial collapse of Mofjellbekken Bridge in Norway. In *Landslides and Engineered Slopes. Experience, Theory and Practice* (ed. Aversa S et al.) CRC Press. 12th Intern. Symp. on Landslides. Napoli, Italy. Ch. 121: 1091–1097.
- [4] Karlsrud K, Heyerdahl H, Kim Y and Hendersen, L. (2015). Sikringstiltak for- og refundamentering av Skjeggestad bruene etter skredet 2 februar 2015. NGF. Geoteknikkdagen 2015. Kap 42. 21 pp.
- [5] Rødvand, L A, Andresen L and Grimstad, G (2019). Case study of a road bridge hit by a landslide in highly sensitive clay. Proceedings of the XVII ECSMGE-2019.
- [6] Fellenius B. 1936, Calculations of the Stability of Earth Dams. Proc. 2nd Intern, Congress of Large Dams (ICOLD). **4**: 445–463.
- [7] Janbu, N (1954). Applications of Composite Slip Surfaces or Stability Analysis. Proc. European Conf. on the Stability of Earth Slopes, Stockholm., **3**: 39–43.
- [8] Bishop, A W (1954). The use of the slip circle in the stability analysis of slopes. Proc. European Conf. Stab. Earth Slopes, Stockholm. **1**:1–13 (and in *Geotechnique*. **V**(1):7.
- [9] Morgenstern N R and Price V E (1965). The Analysis of the Stability of General Slip Surfaces. *Geotechnique*. **15** (): 79–93.
- [10] Spencer E (1967). A Method of Analysis of Embankments assuming Parallel Interslice Forces. *Geotechnique*. **17** (1) 11–26.
- [11] Griffiths D V and Lane P A (1999). Slope stability analysis by finite elements. *Geotechnique*, **49**(3): 387–403.
- [12] NPRA-Norwegian Public Roads Administration. (1997). ZD95C-1-E18 Nordre Vestfold parsell 5B Mofjellbekken bru profil 30152-30370.
- [13] Ladd, C.C., Foot, R., Ishihara, K., Schlosser, F. and Poulos, H.G. (1977). Stress-deformation and strength characteristics. Soa Report. 8th ICSMGE (Tokyo). Proc. **2**: 421–494.
- [14] NGI (Norwegian Geotechnical Institute) (1986). Soil parameters for offshore foundation design. Part I. NGI Report 40013-34 (Kleven, A., Lacasse, S. and Andersen K.H.). 9 April 1986.
- [15] Trimble NovaPoint Geosuite. Version 16.1.5.0.
- [16] Lacasse S, Jostad H P, H.P., L'Heureux J-S, Torgersrud Ø and Sandven R. (2015). Geosuite - A modular software for geotechnical design. Proc. 68th Canadian Geotechnical Conf. GeoQuébec.Can. Geotechnical society.
- [17] Jostad HP and Lacasse S (2015). 3D effects in undrained slope stability analysis of clays. In Winter et al. (eds.) Proc. XVI ECSMGE Edinburg (1573–1578). London: ICE Publishing. DOI:10.1680/ecsmge.60678.
- [18] Azzouz AS and Baling MM (1983). Loaded areas on cohesive slopes. Journal of Geotechnical Engineering, **109**(5): 724–729. ISSN 0733-9410/83/0005-0724/\$01.00. Paper No. 17929.
- [19] Jostad, H P, Fornes, P, Thakur, V (2014). Effect of strain-softening in design of fills on gently inclined areas with soft sensitive clays. In *Landslides in sensitive clays. From Geosciences to Risk management*. Springer, Dordrecht. (305–316).
- [20] NPRA (2018). N200 Veibygging - Technical specification document N200, Norwegian Public Roads Administration (NPRA). Available at <http://www.vegvesen.no/Fag/Publikasjoner/Handboker> (in Norwegian).
- [21] Oset F, Thakur V, Dolva B K et al. (2014). Regulatory framework for road and railway construction on the sensitive clays of Norway. In: *Landslides in sensitive clays. From geosciences to risk management*, ISBN 978-94-007-7079-9, p 343–353.